# Memory in an Excitable Medium: A Mechanism for Spiral Wave Breakup in the Low-Excitability Limit

Flavio H. Fenton,[1,2] Steven J. Evans,[1] and Harold M. Hastings[2]
[1]*Harris Chasanoff Heart Institute, Long Island Jewish Medical Center, New Hyde Park, New York 11042*
[2]*Department of Mathematics, Hofstra University, Hempstead, New York 11549*
(Received 28 May 1999)

The electrophysiology of cardiac tissue is altered during acute myocardial ischemia, making the tissue less excitable but, nonetheless, more susceptible to tachyarrythmias which frequently degenerate to fibrillation within several seconds. The transition from tachycardia to fibrillation is associated with the breakup of spiral waves into multiple offspring, and has been linked to steep restitution (slope $> 1$) of action potential duration (APD). However, restitution curves become so flat during ischemia that this mechanism does not apply. We found that when the response of APD to recent activations is included in a model of excitable media, spiral breakup can occur even when the slope in APD restitutions is $<1$.

PACS numbers: 87.19.Hh

Spiral waves of electrical activity occurring in cardiac tissue are life threatening because they act as high frequency sources of waves which take control over the heart's natural pacemaker and induce tachycardia. Once initiated in the ventricles, tachycardia (VT) usually decays within a few seconds into ventricular fibrillation (VF) [1], a more spatiotemporally disorganized electrical activity leading to sudden cardiac death. Experiments in the heart using simultaneous multi-site electrode mappings have shown that in many cases VF is a consequence of several wandering spiral waves [1,2]. It has also been suggested that the rapid transition from VT to VF can be associated with the breakup of a spiral wave into multiple offspring [3,4]. Over the last decade spiral wave breakup has been studied using models of excitable media ranging from simple generic [5–7] to detailed ionic models with explicit membrane processes which accurately reproduce the cardiac action potential at the single cell level [8–10]. The dynamics and stability of spiral waves obtained with these models can be analyzed in terms of two mesoscopic functions; the restitution of action potential duration (APD) and restitution of conduction velocity (CV) [11,12]. These functions describe how the duration and conduction velocity of a wave depend on the time interval since the previous activation, during which the medium recovers its resting properties. These restitution functions thus reflect the electrophysiological state as well as tissue characteristics. Numerical simulations with different models have shown that steep APD restitution curves (slope $> 1$) can cause slow recovery fronts [3] and APD alternation [4]. Both mechanisms are proarrhythmic, leading to breakup and disorganized electrical activity. Nevertheless, most experimental studies in normal tissue have reported APD restitution curves with slope $< 1$ [13,14]. Therefore it remains unclear whether steep restitutions occur only in diseased tissue [15], different protocols are needed to measure APD restitutions [16], and/or other mechanisms are responsible for spiral wave breakup [12,17]. Furthermore, previous studies have shown that APD restitutions depend not only on the last activation, but in fact upon previous basic cycle lengths (BCLs) [13,16,18–21].

In this Letter, we incorporate in a phenomenological way the effect of BCL history ("memory") into a model for cardiac action potential. This yields APD restitution curves which also depend upon previous BCLs, and provide a new mechanism for spiral wave breakup in the low-excitability limit.

The adaptation of APD to changes in cycle length can be attributed to [18]: (i) nonequilibrium values of the ionic currents (incomplete membrane recovery) and (ii) changes in electrochemical gradients and permeability due to differences in accumulation of intracellular calcium and extracellular potassium at different rates of stimulation. Even though the precise cellular mechanism involving electrical memory is not known in many instances the APD restitution for a given BCL can be fitted by the sum of two exponentials [13,15,18]. Furthermore, Elharrar and Surawicz [13] showed that the two exponential components are almost independent of BCL and thus

$$\mathrm{APD}_t = \mathrm{APD}_{\max} g(\mathrm{BCL}) \times \left[1 - A_1 \exp(-\mathrm{DI}_t/T_1) - A_2 \exp(-\mathrm{DI}_t/T_2)\right]. \quad (1)$$

Here $\mathrm{DI}_t$ is the preceding diastolic interval (the previous cycle length is denoted by $\mathrm{APD}_{t-1}$), $T_i$ and $A_i$ are fitted constants from experimental APD curves [13], and $g(\mathrm{BCL})$ represents the memory ($g = 1$ at large BCL and decreases with decreasing BCL). An explicit formula for $g(\mathrm{BCL})$ can be obtained [13] and used to calculate theoretical APD restitutions at different BCLs (Fig. 1). Note that as the BCL decreases the maximum APD also decreases, flattening the APD restitution curve.

In order to reproduce these APD restitutions in numerical simulations from an ionic model, memory must be

 0031-9007/99/83(19)/3964(4)$15.00 

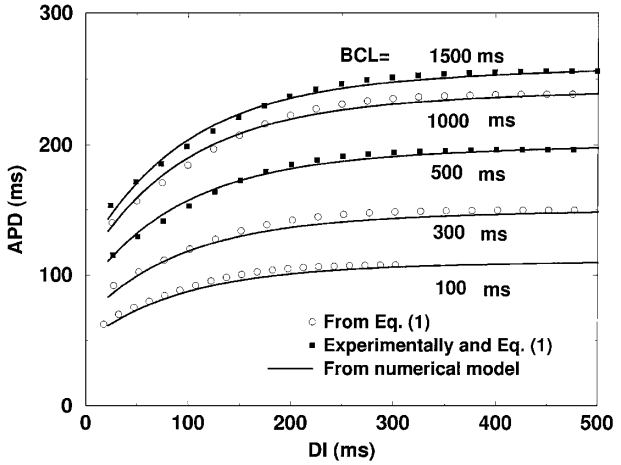


FIG. 1. APD restitutions at five different BCLs. The model equations are integrated using a second order implicit scheme described in Ref. [12]. The minimum diastolic interval was chosen to fit the Luo-Rudy-I CV restitution (see text).

incorporated. The first complex mathematical models used to describe the APD in cardiac tissue [8,9] lacked exchange currents and ignored several time dependent ionic concentrations. As a result they generate APD restitution curves which depend only on the last DI and not on previous cycle lengths. "Second generation" complex ionic models [10] are more robust since they include dynamic ionic concentrations, pump exchangers, and more ionic currents. However, they are not only too slow to simulate in more than one dimension, but also some of their ionic fluxes seem to display unrealistic saturations when periodically stimulated at high frequencies for prolonged times [22].

Therefore we chose to incorporate memory into a simplified ionic model [12], which can trace arbitrary monophasic restitution curves and can reproduce the dynamics of more complex models when fitted to their respective restitution curves. The model consists of three independent currents: $I_{\rm ion} = I_{\rm fi} + I_{\rm so} + I_{\rm si}$. Here $I_{\rm fi}(u;v) = -v(u - 0.13)(1 - u)p/\tau_d$. $I_{\rm fi}$ controls the CV restitution and represents the fast inward current (Na), it is a function of $u$ (the membrane voltage which propagates according to the cable equation [3,4,11]) and a fast gate $v$ given by $\partial_t v = (1 - p)(1 - v)/[\tau_{v1}^-(1 - q)\tau_{v2}^- q] - pv/\tau_v^+$. The APD restitution is controlled by a slow outward current (K) $I_{\rm so}(u) = u(1 - p)/\tau_0 + p/\tau_r$ and a slow inward current (Ca) $I_{\rm si}(u;w) = -w\{1 + \tanh[10(u - 0.85)]\}/2\tau_{\rm si}$ with a slow gate $w$ defined by $\partial_t w = (1 - p)(1 - w)/\tau_w^- - pw/\tau_w^+$. The time constants and the Heaviside functions $p$ and $q$ are further described in [12]. Figure 1 shows how this model reproduces the APD restitution curve at different BCLs after choosing appropriate time constants (Table I). Memory is included as follows. First, convert the time constants responsible for the APD restitution into functions of the cycle length $(bcl)$, which becomes a variable in the model. A least squares method is used to fit the values

TABLE I. Values for the ionic time constants used to obtain the different BCL's. The first part of the table corresponds to "normal" tissue (Fig. 1) and the second part to "ischemic" tissue (Fig. 3).

| | $BCL_{100}$ | $BCL_{300}$ | $BCL_{500}$ | $BCL_{1000}$ | $BCL_{1500}$ |
|---|---|---|---|---|---|
| $\tau_w^+$ | 500 | 720 | 900 | 1110 | 1200 |
| $\tau_w^-$ | 50 | 59 | 60 | 64 | 70 |
| $\tau_{\rm si}$ | 20.7 | 37 | 55 | 76.3 | 90.5 |
| $\tau_r$ | 24 | 42 | 62 | 85 | 100 |
| $\tau_r$ | 112 | 164 | 203 | 257 | 275 |
| $\tau_d$ | 0.35 | 0.32 | 0.29 | 0.23 | 0.17 |

in Table I. In order to obtain monotonic functions of $bcl$ over the range 0–1500 ms, cubic polynomials were used to represent $\tau_{\rm si}$ and $\tau_r$ and fourth order polynomials were used to represent $\tau_w^+$ and $\tau_w^-$. Next, add an extra variable $T$ that tracks the time of the last activation and is used to update $bcl$ in response to sudden changes in cycle length.

The response of APD adaptation to abrupt changes in BCL depends upon the direction of the change. After the BCL is abruptly shortened in healthy tissue, APD decreases rapidly at first, and later decreases more slowly reaching a new steady state after many beats [13,21]. On the other hand, after an increase in BCL, the APD adapts more smoothly and takes several beats longer to reach its new larger steady state value [13,21]. Hysteresis in adaptation to BCL and the dynamical link between APD restitutions at different BCLs is modeled to first approximation with a simple piecewise linear equation which updates the $bcl$.

$$bcl = \begin{cases} \alpha_1 bcl + (1 - \alpha_1)T & \text{if } bcl \le T\,, \\ \alpha_2 bcl + (1 + \alpha_2)T & \text{otherwise.} \end{cases} \qquad (2)$$

The CV restitution curve has not been studied as broadly as its APD counterpart. We therefore chose to fit the CV curve to one obtained from the "first generation" model which has the most accurate Na current, i.e., the Luo-Rudy-I (LR-I) model [9,12] ($\tau_{v1}^- = \tau_{v2}^- = 18.18$, $\tau_v^+ = 10$, $\tau_0 = 12.5$, and $\tau_d = 0.172$). Furthermore, we left the CV independent of BCL since experiments have shown that in normal tissue, cycle length does not significantly affect maximum longitudinal or transverse velocity [23].

Using polynomial representations of the time constants in Table I, a LR-I CV restitution, and an initial BCL 1500 ms, a spiral wave was initiated by a broken plane wave [3,12] (equivalent to induction by a cross-field stimulation in real tissue). The spiral wave tip initially followed a linear core trajectory of about 2 cm with a period of ≈150 ms. As the spiral turned, both the cycle length and the rotational period decreased as expected [21], resulting in a shorter period of ≈60 ms with a linear core of ≈5.5 mm. The final period of rotation was shorter than that observed experimentally. This follows from the small minimum diastolic interval given by the

LR-I C restitution curve and the relatively short $APD_{max}$ obtained from Eq. (1) at BCL smaller than 200 ms. We checked numerically that increasing either of these increases the rotational period. During dynamical BCL adaptation produced by the spiral wave while rotating, oscillations of APD where observed and even transient breakup [Figs. 4(a)–4(c)]. New spiral waves are not formed because the APD remains large at this stage causing the broken ends to recombine, much in the same way as an obstacle too small compared to the wavelength is unable to induce breakup [24].

When the cardiac tissue suddenly lacks enough oxygen it becomes ischemic, arrhythmias are generated almost immediately and frequently culminate in VF [25,26]. We therefore proceeded to investigate if the ischemic electrophysiology could increase the amplitude in APD oscillations during spiral cycle length adaptation and be a cause of spiral wave breakup at this regime.

During ischemia the electrophysiology of the cardiac tissue is altered in several ways: (i) $APD_{max}$ decreases and the restitution of action potential becomes flatter [25]; (ii) due to a decrease in resting membrane potential, the maximum upstroke velocity of action potential decreases, lowering the maximum CV [21]; (iii) cellular coupling, and thus upstroke velocity, becomes dependent upon cycle length, making CV a function of BCL [20] unlike the case of normal tissue; (iv) APD adaptation to a sudden decrease in BCL becomes smooth and seems almost linear [19].

One reason for flattening of APD restitution is the smaller contribution from the calcium currents [25]. Ischemia can then be included by eliminating $I_{si}$, which flattens the APD restitution curves [12,27], and makes them depend only on $\tau_r$. A decrease in $CV_{max}$ can be achieved by increasing $\tau_v^+$ (we use $\tau_v^+ = 3.5$). The subsequent changes in CV restitution as a function of BCL arise from making the sodium conduction ($\tau_d$) a function of BCL and setting $\tau_{v2}^- = 88$. Finally, the slower adaptation to BCL changes is achieved by increasing $\alpha_1$ in Eq. (2) (Fig. 2). Figure 3 shows the flat APD restitution obtained with the constants of Table I.

When a spiral wave is initiated using the ischemic parameters, it follows a similar period shortening as in "normal" tissue. Breakup due to slow recovery fronts is also observed during the first rotations, even though the slope in the APD restitutions is less than 1. However, as in the normal case, the APD is too large and the breakup is transient. Nevertheless, after approximately 18 rotations the BCL has become so short that excitability is significantly reduced, causing spiral breakup.

More precisely, as the cycle length shortens, the spiral wave gets close to a regime of very low excitability in which the radius of rotation diverges and spiral tips retract [6,7], with speed increasing as excitability decreases [7]. When the spiral wave tip meanders, it can quickly turn in a small region of extremely weak excitability resulting in a fast wave contraction. Such rapid contraction can leave behind a small "voltage droplet" as shown in Figs. 4(d)–4(f). This is probably a generic phenomena in media with very low excitability [28]. However, in our case, because of the dynamic cycle adaptation, the droplet can find excitable regions and propagate [Figs. 4(g)–4(i)] producing multiple waves. The result is identical in effect to a premature stimulus following in the wake of a wave. We note that the time it takes for a spiral to reach breakup in this mechanism ($\approx$4 s) agrees with the lifetime of Wiggers stage I [1] before VF goes into full disorganization (Wiggers stage II). This breakup mechanism may be amplified when one considers the enhancement in dispersion of repolarization occurring during ischemia.

In summary, our results show that spiral wave breakup can be induced even with flat APD restitutions, as long as the dynamic effects of tissue memory and sufficiently large changes in BCL are considered. Note that "slope $<$ 1" criteria for stability reflect only the effect of small perturbations from equilibria, and BCL starts far from an attractor and appears to fluctuate chaotically during the approach as well as on the attractor.

In addition, it will be desirable to check the validity of Eq. (1) at low BCLs and to measure experimental CV and APD restitutions at different BCLs in

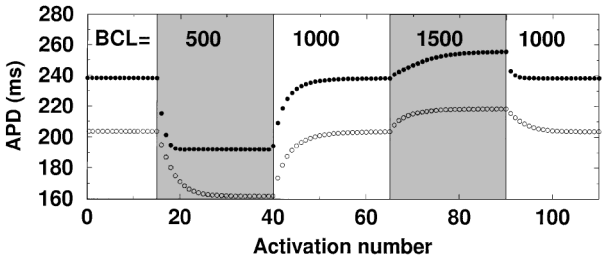


FIG. 2. Adaptation to sudden changes in BCL. The BCL was changed from 1000 to 500 to 1000 to 1500 and back to 1000 ms. Bullets correspond to "normal tissue" ($\alpha_1 = 0.4$) and open circles to "ischemic" ($\alpha_1 = 0.7$). In both cases $\alpha_2 = 0.8$.

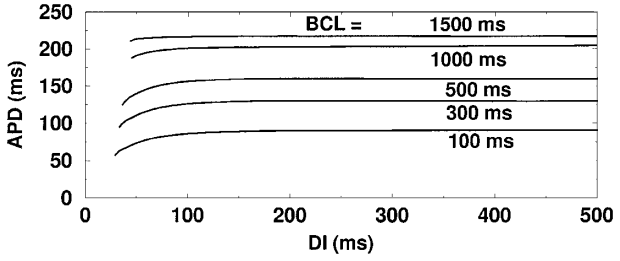


FIG. 3. Simulated APD restitution curves at different BCLs during ischemia. The constant APD was chosen by taking the average of $APD_{max}$ and $APD_{min}$ from the "normal" case (Fig. 1). This approach seems to agree with experimental APD restitutions [25]. The small slopes [27] are $<$0.65.

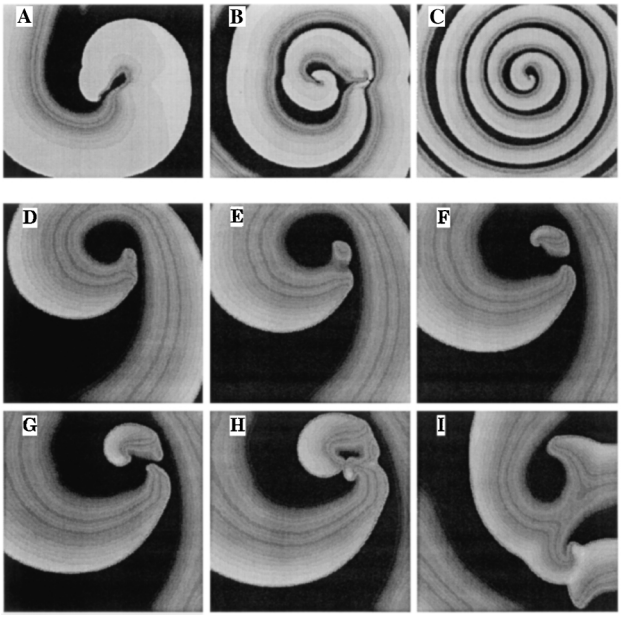


FIG. 4. Normal tissue (the large size of 17 × 17 cm was chosen to model BCL adaptation), (A) spiral wave after first rotation ($t = 200$ ms), (B) unsuccessful breakup ($t = 1.1$ s), (C) final stable spiral ($t = 3$ s). Ischemic tissue (size 8.5 × 8.5 cm), (D)–(I) generation of a "voltage droplet" resulting in multiple waves ($t = 4.08, 4.09, 4.1, 4.11, 4.13, 4.5$ s).

ischemic tissue so they can be included in the model. Equation (2) might be expanded by including a longer history of previous activations in order to better describe adaptation to changes in cycle length as well as to reproduce observed small oscillations in APD [13,21] which may have important effects.

We acknowledge support from NIH SCOR in Sudden Cardiac Death 1PL50HL-52319, the Chasanoff Endowment of LIJ Medical Center, the Long Island Heart Council, the Louise and Michael Stein Philanthropic Fund, the Rosalyn S. Yalow Foundation for Biomedical Research, CPI, Medtronic, and NU-ASCC.

[1] P. S. Chen *et al.*, Chaos **8**, 127 (1998).
[2] M. J. Janse, Chaos **8**, 149 (1998).
[3] M. Courtemanche and A. Winfree, Int. J. Bifurcation Chaos Appl. Sci. Eng. **1**, 431 (1991); M. Courtemanche, Chaos **6**, 579 (1996).
[4] A. Karma, Phys. Rev. Lett. **71**, 1103 (1993).
[5] FitzHugh, Biophys. J. **1**, 445 (1961); J. J. Tyson and J. P. Keener, Physica (Amsterdam) **32D**, 327 (1988).
[6] A. S. Mikhailov and V. S. Zykov, Physica (Amsterdam) **52D**, 379 (1991); A. Karma, Phys. Rev. Lett. **66**, 2274 (1991).
[7] A. Karma, in *Growth and Form*, edited by M. B. Amar *et al.* (Plenum Press, New York, 1991).
[8] G. W. Beeler and H. Reuter, J. Physiol. **268**, 177 (1977); D. Noble, J. Physiol. **160**, 317 (1962).
[9] C. Luo and Y. Rudy, Circ. Res. **68**, 1501 (1991).
[10] C. Luo and Y. Rudy, Circ. Res. **74**, 1071 (1994); D. DiFrancesco and D. Noble, Philos. Trans. R. Soc. London B **307**, 353 (1985).
[11] M. Courtemanche, L. Glass, and J. P. Keener, Phys. Rev. Lett. **70**, 2182 (1993); A. Karma, Chaos **4**, 461 (1994); M. Courtemanche, Chaos **6**, 579 (1996).
[12] F. Fenton and A. Karma, Chaos **8**, 20 (1998); Phys. Rev. Lett. **81**, 481 (1998).
[13] V. Elharrar and B. Surawicz, Am. J. Physiol. **244**, H782 (1983).
[14] See, for example, Refs. [13,16,19,25–27] in [16].
[15] H. S. Karagueuzian *et al.*, Circulation **87**, 1661 (1993).
[16] M. L. Koller, M. L. Riccio, and R. F. Gilmour, Am. J. Physiol. **275**, H1635 (1998).
[17] V. N. Biktashev, A. V. Holden, and H. Zhang, Philos. Trans. R. Soc. London A **347**, 611 (1994); A. Panfilov and J. Keener, Physica (Amsterdam) **84D**, 545 (1995); F. Fenton, S. Evans, and H. M. Hastings (to be published).
[18] M. R. Boyett and B. R. Jewell, J. Physiol. **285**, 359 (1978).
[19] D. S. Rosenbaum *et al.*, Circulation **84**, 1333 (1991).
[20] Y. Hiramatsu *et al.*, Circ. Res. **65**, 95 (1989).
[21] M. R. Franz *et al.*, Clin. Invest. **82**, 972 (1988).
[22] A. Xu and M. R. Guevara, Chaos **8**, 157 (1998).
[23] M. J. Reiter *et al.*, Circulation **96**, 4050 (1997).
[24] J. M. Starobin *et al.*, Biophys. J. **70**, 581 (1996); J. Jalife *et al.*, Chaos **8**, 79 (1998).
[25] P. Taggart *et al.*, Circulation **94**, 2526 (1996).
[26] K. Mizumaki *et al.*, PACE **16**, 1656 (1993).
[27] In low excitability and short DI's there is a strong coupling between APD and CV restitutions; the slope is a consequence of smaller APD's due to slower upstrokes.
[28] We have found "voltage droplets" in other models, for example use ($\epsilon = 0.2$, $M = 4$, $v^* < 0.2$) in the model of Ref. [4]. For these parameters, the constant excitability is so low that voltage droplets are too small to reexcite the surrounding tissue and they die out.